Biomaterials Science: Processing, Properties and Applications III.
Edited by Susmita Bose, Amit Bandyopadhyay and Roger Narayan.

INFLUENCE OF TANTALUM AND TUNGSTEN DOPING ON POLARIZABILITY AND BIOACTIVITY OF HYDROXYAPATITE CERAMICS

Jharana Dhal[1], Susmita Bose[2] and Amit Bandyopadhyay[2]
W. M. Keck Biomedical Materials Research Lab
[1]Department of Physics
[2]School of Mechanical and Materials Engineering
Washington State University, Pullman, WA, USA.
E-mail: amitband2010@gmail.com

ABSTRACT

We examined the effect of doping of pentavalent tantalum (Ta) and hexavalent tungsten (W) on the polarizability of hydroxyapatite (HAp) ceramic. Doping decreased the concentration of HAp while increased the concentration of other phases such as β-TCP and α-TCP. Doped HAp ceramics had less stored electrical charge density compared with pure HAp. Comparing the activation energies of depolarization and different phase percentages in tungsten-doped samples, we found that stored charge decreases due to the resistance in ion migration through different phases. However, similar mechanism did not explain a decrease in stored charge density in tantalum-doped HAp. Our results demonstrate the influence of dopant chemistry on store charge density and *in vitro* bone cell biology of HAp ceramics.

INTRODUCTION

Hydroxyapatite (HAp; $Ca_{10}(PO_4)_6(OH)_2$) ceramics has been used as to coat orthopedic or dental implants because of its structural and compositional similarities with bone tissue [1-3]. Although HAp bonds strongly with natural bone tissue and helps stabilization of implant *in vivo*, inferior osteogenic capacity and poor mechanical properties of synthetic HAp compared with bone limits the use of HAp [4]. To improve the bioactivity of HAp ceramics, several methods are reported including: (1) polarization of HAp [5-9], (2) doping with metal cations [7, 10-12], and (3) mixing of HAp with tricalcium phosphate (TCP) to form biphasic compositions [13].

Bone exhibits piezoelectric effects (mechanical stress generates internal electrical charge) that help in bone formation [14]. Bassett et al. [15, 16] used polarization to induce surface charge that improve osseo-integration in HAp and enhanced bone formation [17]. Polarization of HAp was attributed to the proton migration of –OH group along the c-axis of the hexagonal crystal structure [18] or simultaneous migration of O^{2-} and H^{+} [19]. The polarization developed surface charge on HAp whose polarity could influence the growth of bonelike apatite crystals and bone growth on the polarized HAp in simulated body fluid (SBF) [5, 20].

Trace elements that are naturally present in bone but absent in synthetic HAp have been added to HAp to improve its bioactivity. For example, substitution of divalent or trivalent metal ions in HAp improved the structural stability and *in vitro* biocompatibility properties of HAp [10, 11, 21-24]. In our previous studies, we have doped HAp with Mg, Zn and Sr in single, binary and ternary combinations and studied under electrical polarization treatment [7]. We have found that combined doping of 1 % Mg and 1 % Sr by weight with HAp increased the charge storing ability to maximum among other dopants by inhibiting the high temperature decomposition of HAp [25]. Several other studies provided evidence of increase in bioactivity of HAp when doped with various cations [7, 10, 24]. Doping could change structure, microstructure, and surface properties in HAp.

Though increasing valency of doped cations improved the bioactivity of HAp, cation having a valency greater than four has not been doped with HAp. Of those few studies where HAp was doped with di-, tri or tetra-valent cations, effect of polarization on the bioactivity of doped HAp was not considered in all cases. The aim of our study was to measure the polarizability and bioactivity of HAp doped with hexavalent tungsten and pentavalent tantalum. We hypothesize that tungsten and bioactive tantalum [26] will influence polarizability and bioactivity of HAp. Influences of doping and polarization on cell–material interactions were investigated *in vitro*. Human osteoblast cells were used and the bioactivity was evaluated.

EXPERIMENTAL PROCEDURE

Sample preparation and characterization: Two different compositions of HAp for each dopant were prepared by doping 0.25% and 0.5% by weight of WO_3 (99.99%, Alfa Aesar) or Ta_2O_5 (99.95%, Alfa Aesar) with HAp (Berkeley Advanced Biomaterials, CA). Additionally, pure β-TCP and 0.5wt% WO_3 doped β-TCP were also used. A mixture of HAp and WO_3 or Ta_2O_5 were ball-milled in ethanol media at 70 rpm for 24 h, dried in an oven at 80 °C for 72h and uniaxially pressed to obtain disk samples. Disk samples were further pressed isostatically at 345 MPa for 5 minutes and sintered at 1250 °C for 2 h in air to form the disk with 10.4 mm in diameter and 1.2 mm in thickness. The apparent density of each composition was measured by the Archimedes' method and reported as relative density by normalizing with the theoretical density of HAp (3.16 g cm^{-3}). Phases in each composition were analyzed by X-ray diffractometer (Siemens D500 Kryatalloflex, Siemens Corporation, NY) using copper Kα radiation with a Ni filter at 30 kV and 35 mA in 2θ ranges between 20 and 60 degrees. The weight fractions (W) of different phases in sintered and doped samples were determined using Equation 1 [27], where I is the highest intensity of XRD peaks.

$$W_{calculated\ phase} = \frac{I_{calculated\ phase}}{I_{calculated\ phase} + \sum I_{other\ phases}} \qquad (1)$$

Electro-thermal polarization and TSDC measurement: Sintered samples were polarized and the polarization conditions were investigated with a thermally stimulated depolarization current (TSDC) technique [28]. Briefly, the disc samples were coated with silver paint on both sides, baked for one hour at 200 °C, and sandwiched between a pair of platinum plates connected with silver wires. A d.c. voltage was applied through silver wires using a picoammeter (Model 6487, Keithley Instruments Inc., OH). Samples were heated with a controlled heating rate of 5°C min^{-1} from room temperature to polarization temperature (T_p) of 400 °C and kept at T_p for 1h. The doped samples of different compositions were kept in d.c. electric field (E_p) of 2kVcm^{-1} for 1h at T_p and cooled down to room temperature while keeping the applied field E_p still on. The polarized samples were heated at a rate of 5 °C min^{-1} from room temperature to 550 °C and TSDC was measured using the picoammeter.

Stored charge (Q_p) and activation energy for dipole relaxation (E_{dr}) were estimated from the TSDC curve. Arrhenius plots were obtained from TSDC spectrum assuming single Debye type dipole relaxation. Equation 2 was used to estimate the charge storage and Equation 3 was used to calculate activation energy for dipole relaxation [18].

$$Q_p = \frac{1}{\beta}\int J(T)\, dT \qquad (2)$$

$$\ln(\tau) = \frac{E_{dr}}{kT} + \ln(\tau_0) \quad (3)$$

Where $J(T)$ is the depolarization current density at temperature T, β is the heating rate during TSDC measurement. The dipole relaxation time (τ) at temperature T is expressed by Equation 3 [9, 18].

$$\tau = \frac{1}{\beta(T)J(T)}\int J(T)dT = \frac{Q_p(T)}{J(T)} \quad (4)$$

In vitro study: *In vitro* studies were carried out on pure and doped HAp (polarized and unpolarized) following method outlined in reference 5 [5]. HAp sample doped with 0.5 % WO_3 were selected for *in vitro* study because of its high charge storing ability compared to other two doping compositions. For tantalum doped samples, HAp with 0.25% Ta_2O_5 were selected because of high percentage of HAp phase in these samples after sintering. Samples for *in vitro* study were polarized with and without silver coating on both sides. The silver coatings of samples were removed by mechanical polishing and sonicating in deionized water. In polarized doped samples, the negatively polarized surfaces were denoted as the N surfaces and the positively polarized surfaces are denoted as P-surfaces. Surfaces without polarization were designated as O-surface.

Human fetal osteoblast cells (hFOB) were used to examine the interaction with doped and pure HAp samples prepared for *in vitro* study. Cells, derived from immortalized human osteoblastic cell line established from human bone tissue [29, 30], were cultured in culture plate for 10 days. These cells were seeded on sterile pure and doped HAp in a plate with 24 wells to which 1 ml of DMEM media enriched with 10% fetal bovine serum was added. These samples were incubated at 37 °C in air with 5% CO_2. The cell culture media was changed every alternate day. These incubated samples were used for cell proliferation study and cell morphology.

Cell proliferation was measured in triplicates on the WO_3 doped samples incubated for 3 and 7 d by performing MTT assay (Sigma Inc., St Louis, MO) whereas Ta_2O_5 doped samples were incubated additionally 11 d. The incubated cells were transferred to a new 24-well cell culture plate to prevent the contribution of cells grown on the plastic surface of the original 24 well plate to the assay result. MTT was dissolved in phosphate-buffered saline (PBS) solution to achieve concentration of 5 mg mL^{-1}, filtered, and sterilized. A 50μL MTT was diluted into 450μL of DMEM culture media enriched with 10% fetal bovine serum. The diluted MTT was added to each sample in 24-well plates and incubated for 2 h at 37 °C to form formazan by mitochondrial dehydrogenase. The formazan crystals were dissolved in 500μL of solution made up of 10% Triton X-100, 0.1N HCl, and isopropanol. The optical density of the solution in each well was measured at a wavelength of 570 nm in triplicates by transferring 100 μL from each well to well in 96-well plates.

Cell morphology was measured by SEM on samples incubated for 3, 7, and 11 d. The cultured samples were rinsed with 0.1M PBS and fixed overnight at 4 °C with 2% paraformaldehyde and 2% glutaraldehyde in 0.1 M cacodylate buffer. Fixed samples were treated with 2% osmiumtetroxide (OsO_4) for 2 h at room temperature, dehydrated three times in an ethanol series (30%, 50%, 70%, 95% and 100%), and dried using hexamethyldisilane (HMDS). Dried samples were mounted on aluminum stubs, coated with gold, and observed under FESEM.

Statistical Analysis: Each analysis was done in triplicates. Statistical analysis was done on results from MTT assay using Student's t-test where a p-value less than 0.05 considered significant.

RESULTS

Phase analysis: The XRD results indicate the presence of β-TCP and small fraction of HAp in all WO_3 and Ta_2O_5 doped samples (Table 1). However α-TCP was also found in 0.5% TA_2O_5 doped specimens. The characteristics peaks of HAp, β-TCP, and α-TCP in all samples match well with JCPDS file numbers 09-0432 (HAp), 09-0169 (β-TCP) and 09-0348 (α-TCP). Increasing WO_3 concentration to 0.5wt% HAp phase decreases to 8% and 92% β-TCP. No peaks associated with tantalum or tungsten phases were detected in doped HAp samples. The results also indicate that 0.5% doped β-TCP sample have β-TCP and $Ca_{4.26}W_{10}O_{30}$ phases. Characteristics peaks of β-TCP and $Ca_{4.26}W_{10}O_{30}$ in doped β-TCP samples match with the JCPDS number 09-0169 for β-TCP, and 83-1046 for $Ca_{4.26}W_{10}O_{30}$. β-TCP doped with 0.5% WO_3 contained about 87 wt% of β-TCP and 13 wt% of $Ca_{4.26}W_{10}O_{30}$ phase. Relative density of pure and doped HAp are also reported in Table 1.

Thermal depolarization: The TSDC of all samples increased as a function of temperature after 200 °C and reached a maximum current density before started to decrease (Fig. 1 and Fig. 2). The maximum current density varied among all samples. However, the highest maximum current density was found for pure HAp. Maximum current density, J_{max}, of 0.5% doped sample was higher than 0.25 wt.% for both WO_3 and Ta_2O_5 doped sample. But the Ta_2O_5 doped samples shows lower J_{max} and stored charge (Q_p) compared to pure HAp and WO_3 doped. The stored charge (Q_p) and activation energy of depolarization of all samples are presented in Table 1.

In vitro cell-material interaction: The MTT colorimetric assay indicates that O-, N-, and P-surface in doped samples show higher cell proliferation than pure HAp (Figure 3 and 4) for both WO_3 and Ta_2O_5 doped HAp. Cell proliferation was significantly higher on N- and P-surfaces compared to O-surface for both group of doped HAp samples. FESEM images of pure HAp, O-surface, N-surface and P-surface samples of Ta_2O_5 and WO_3 dopes HAp incubated in hFOB cells for 11 d shows that the P- and N-surfaces have higher surface coverage by cells than HAp and O-surface (Figure 5 and 6). Whereas the O-surface has confluent and higher concentration of cells compared to pure HAp surface (Figure 5 and Figure 6).

DISCUSSION

Effect of doping on HAp structure: High fraction of β-TCP phase in doped samples indicates the structure of HAp doped with both cations is unstable. This instability is attributable to high temperature sintering and lattice strain. The lattice strain is attributed to a difference in cationic radius and oxidation state of tungsten (0.69 Å, W^{6+}; 0.65 Å, Ta^{+5}) compared to calcium (0.99 Å, Ca^{2+}). XRD results indicate an absence of peaks corresponding to phases of tungsten or tungsten compounds and tantalum or tantalum compounds. Considering this result and smaller size of tungsten and tantalum ion compared to calcium, we hypothesize that W^{6+} and Ta^{5+} ion replaces the Ca^{2+} in the lattice. Similar results were also reported on Ta substituted HAp thin films [23], where Ta^{5+} was suggested to replaces Ca^{2+} ion in HAp structure. The charge compensation could occur by Ca^{2+} vacancy or due to the presence of excess O^{2-}. The Ca^{2+} might be favoring the lower Ca/P ration TCP formation.

Comparison of electrical polarizability: Activation energy (E_{dr}) and stored charge (Q_p) can be used to examine the mechanism of polarization that is similar to mechanism of dielectric relaxation. The activation energy of depolarization by proton rotation is within 0.016 to 0.630

eV with maximum stored charge as 0.55 μC cm^{-2} [18, 31]. The activation energy for H^+ migration along the OH^- chain in the pure HAp is 0.66 ± 0.1 eV [32]. The activation energy corresponding to OH^- diffusion is approximately 2 eV [18]. Comparing activation energies of HAp and 0.25wt% WO_3 suggests that the polarization and depolarization in doped HAp could be primarily due to the proton migration along the -OH chain of HAp phase [18, 32]. Proton migration mechanism didn't explain the change in stored charge with WO_3 dopant concentration and higher activation energy of 0.5wt% WO_3 doped HAp compared to pure and 0.25wt% WO_3 doped HAp. From activation energy of β-TCP and 0.5wt% WO_3 doped β-TCP, it was suggested that the size difference and coordination number of W^{6+} compared to Ca^{2+} cause different structural parameters for doped HAp and doped β-TCP than pure samples. This structural parameter difference possibly result in the activation energy difference between WO_3 doped HAp [33]. The polarization charge (Q_p) in WO_3 doped samples could be explained by ion migration in different phases [33]. The decreases the polarization charge with doping and increase in polarization charge with increasing dopant concentration was attributed to hindrance in ion migration in one phase due to the presence of secondary phases which explains the order of polarization charge value: HAp> 0.5wt% WO_3+HAP > 0.25% WO_3+HAp [33].

The activation energy of Ta_2O_5 doped HAp suggest a similar mechanism as that in WO_3 doped HAp. But proton migration mechanism didn't explain the increase in stored charge with increase in Ta_2O_5 concentration. Other phases, in addition to HAp, could also contribute to the polarization and charge storage in Ta_2O_5 doped HAp as it did in WO_3 doped HAp. But similar argument can't explain a significant drop in stored charge in case of Ta_2O_5 doped HAp compared to pure HAp and a higher stored charge in 0.5% Ta_2O_5 doped HAp compared with 0.25% Ta_2O_5 doped HAp. As 0.5% Ta_2O_5 doped HAp has three kind of phases HAp, β-TCP and α-TCP, this composition of sample should show lower stored charge compared to 0.25% Ta_2O_5 doped HAp. Hence there might be a different mechanism involved in polarization of Ta_2O_5 doped HAp. More study is needed to understand the mechanism of Ta_2O_5 doped HAp.

Bioactivity: Enhanced cell coverage in P- and N-surfaces in WO_3- or Ta_2O_5-doped samples can be attributed to higher surface energy. Surface energy is directly proportional to surface charge. More surface energy leads to higher wettability [34]. Higher wettability supports better cell adhesion and spreading. Higher cell spreading on O-surface samples compared to pure HAp indicates that doping with WO_3 and Ta_2O_5 improved bone cell-materials interaction. Possible explanations for improved bioactivity can be a change in surface chemistry or surface energy due to change in microstructure and different charge state of tungsten and tantalum than calcium on the surface. These factors can influence the interaction of certain proteins such as vitronectin / or collagen, and help osteoblast cell adhesion [35]. Improved cell adhesion leads to higher bioactivity. Results from SEM images are further supported by the MTT data. After 3 and 7 day of incubation, cell proliferation followed the order: N-surface> P-surface> O-surface> pure HAp. Further research is needed to understand the *in vivo* response of these materials with and without surface charge.

CONCLUSIONS

Doping with pentavalent tantalum and hexavalent tungsten increased the bioactivity of HAp. Polarization further enhanced bone cell adhesion and proliferation. We have demonstrated that polarization in WO_3 doped HAp samples were contributed by both HAp and β-TCP phases. Polarization in doped HAp phase was attributed to primarily proton migration in –OH column. However, polarization in doped β-TCP phase was attributed to the migration of O^{2-} or Ca^{2+} ion. A difference in charge stored between WO_3 doped sample and pure HAP as well as the different trend of store charge with increasing dopant concentration is attributed to hindrance in ion

migration. A hindrance in ion migration could occur due to unavailability of appropriate neighboring vacant site due to the presence of dissimilar phases. But using the similar principle couldn't explain the mechanism of polarization in T_2O_5 doped sample. Further study is needed to explain the polarization mechanism in Ta_2O_5 doped HAp.

ACKNOWLEDGEMENTS
Authors like to acknowledge financial support from the NIH-NIBIB to carry out the *in vitro* cell biology work under the R01 grant (PI- Susmita Bose).

REFERENCES

[1] M. Vallet-Regi, J.M. Gonzalez-Calbet, Progress in Solid State Chemistry, 32 (2004) 1-31.
[2] M. Jarcho, Clinical Orthopaedics and Related Research, 157 (1981) 259-278.
[3] P. Ducheyne, J.M. Cuckler, Clin. Orthop. Relat. Res, 276 (1992) 102-114.
[4] A.J. Salgado, O.P. Coutinho, R.L. Reis, Macromolecular Bioscience, 4 (2004) 743-765.
[5] S. Bodhak, S. Bose, A. Bandyopadhyay, Acta Biomaterialia, 5 (2009) 2178-2188.
[6] S. Bodhak, S. Bose, A. Bandyopadhyay, Acta Biomaterialia, 6 (2010) 641-651.
[7] S. Bodhak, S. Bose, A. Bandyopadhyay, Journal of the American Ceramic Society, 94 (2011) 1281-1288.
[8] H. Takeda, Y. Seki, S. Nakamura, K. Yamashita, Journal of Materials Chemistry, 12 (2002) 2490-2495.
[9] Y. Tanaka, T. Iwasaki, M. Nakamura, A. Nagai, K. Katayama, K. Yamashita, Journal of Applied Physics, 107 (2010) 014107.
[10] T.J. Webster, C. Ergun, R.H. Doremus, R. Bizios, Journal of Biomedical Materials Research, 59 (2002) 312-317.
[11] W. Xue, J.L. Moore, H.L. Hosick, S. Bose, A. Bandyopadhyay, W.W. Lu, K.M.C. Cheung, K.D.K. Luk, Journal of Biomedical Materials Research Part A, 79A (2006) 804-814.
[12] A. Bandyopadhyay, E.A. Withey, J. Moore, S. Bose, Materials Science and Engineering: C, 27 (2007) 14-17.
[13] S. Tarafder, S. Bodhak, A. Bandyopadhyay, S. Bose, Journal of Biomedical Materials Research Part B: Applied Biomaterials, 97B (2011) 306-314.
[14] E. Fukada, I. Yasuda, J. Phys. Soc. Japan, 12 (1957) 1158-1162.
[15] C.A.L. Bassett, R.O. Becker, Science, 137 (1962) 1063-1064.
[16] C.A.L. Bassett, R.J. Pawluk, R.O. Becker, Nature, 204 (1964) 652-654.
[17] M. Ohgaki, T. Kizuki, M. Katsura, K. Yamashita, Journal of Biomedical Materials Research, 57 (2001) 366-373.
[18] S. Nakamura, H. Takeda, K. Yamashita, Journal of Applied Physics, 89 (2001) 5386 - 5392.
[19] M. Ueshima, S. Nakamura, K. Yamashita, Advanced Materials, 14 (2002) 591-595.
[20] K. Yamashita, N. Oikawa, T. Umegaki, Chemistry of Materials, 8 (1996) 2697-2700.
[21] C. Capuccini, P. Torricelli, F. Sima, E. Boanini, C. Ristoscu, B. Bracci, G. Socol, M. Fini, I.N. Mihailescu, A. Bigi, Acta Biomaterialia, 4 (2008) 1885-1893.
[22] S.J. Kalita, H.A. Bhatt, Materials Science & Engineering C-Biomimetic and Supramolecular Systems, 27 (2007) 837-848.
[23] S. Kannan, J.H.G. Rocha, S. Agathopoulos, J.M.F. Ferreira, Acta Biomaterialia, 3 (2007) 243-249.
[24] T.J. Webster, E.A. Massa-Schlueter, J.L. Smith, E.B. Slamovich, Biomaterials, 25 (2004) 2111-2121.
[25] S. Bodhak, S. Bose, A. Bandyopadhyay, Materials Science and Engineering: C, 31 (2011) 755-761.
[26] V. Balla, S. Bose, N. Davies, A. Bandyopadhyay, JOM, 62 (2010) 61-64.
[27] R. Kumar, P. Cheang, K.A. Khor, Journal of Materials Processing Technology, 113 (2001) 456-462.
[28] C. Bucci, R. Fieschi, G. Guidi, Physical Review, 148 (1966) 816 - 823.
[29] S.R. Winn, G. Randolph, H. Uludag, S.C. Wong, G.A. Hair, J.O. Hollinger, Journal of Bone and Mineral Research, 14 (1999) 1721-1733.

[30] S.S. Banerjee, S. Tarafder, N.M. Davies, A. Bandyopadhyay, S. Bose, Acta Biomaterialia, 6 (2010) 4167-4174.
[31] M.I. Kay, R.A. Young, A.S. Posner, Nature, 204 (1964) 1050-1052.
[32] G.C. Maiti, F. Freund, Journal of the Chemical Society, Dalton Transactions, (1981) 949-955.
[33] J. Dhal, G. Fielding, S. Bose, A. Bandyopadhyay, J. Biomed. Mater. Res. Part B, 100B (2012) 1836-1845.
[34] D. Aronov, M. Molotskii, G. Rosenman, Appl. Phys. Lett., 90 (2007) 104104 - 104103.
[35] T.J. Webster, C. Ergun, R.H. Doremus, R.W. Siegel, R. Bizios, Journal of Biomedical Materials Research, 51 (2000) 475-483.

Table 1. Activation energy and charge stored in samples prepared at different conditions[a].

Sample Information	Apparent Density[b] (%)	Charge stored ($\mu C/cm^2$)	Polarizing field (kV/cm)	Activation Energy (eV)	% of HAp phase	% of β-TCP phase	% of α-TCP phase
HAp	93.10 ± 1.12	629.6	2	0.78	100	0	0
HAp + 0.25 wt% Ta_2O_5	93.20 ± 2.20	69.78	2	0.66	19	81	0
HAp + 0.5 wt% Ta_2O_5	94.30 ± 1.10	87.4	2	0.63	9	58	33
HAp + 0.25 wt% WO_3	93.75 ± 2.21	248.7	2	0.65	35	65	0
HAp + 0.5 wt% WO_3	94.29 ± 1.26	569.9	2	0.82	8	92	0
β-TCP	94.1 ±1.1	343.2	2	1.1	0	100	0
β-TCP+0.5wt% WO_3	93.5 ± 1.3	723.2	2	0.89	0	87	0

[a] All samples are sintered at 1250 °C for 2h and polarized at 400 °C for 1h
[b] Apparent density is calculated with reference to the theoretical density of HAp, i.e., 3.16g cm^{-3}. The data is reported as average with one standard deviation calculated over 3 samples.

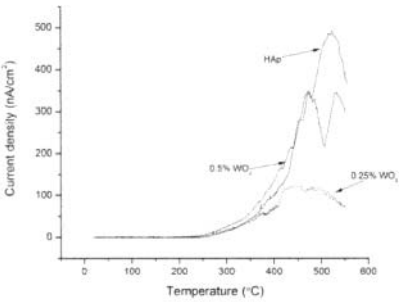

Figure 1. TSDC curve for WO_3 doped HAp polarized at 400 °C by an electric field of 2kV/cm for 1h.

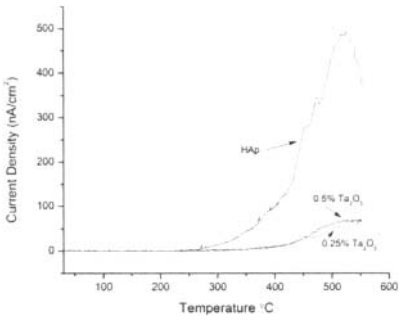

Figure 2. TSDC curve for Ta_2O_5 doped HAp polarized at 400 °C by an electric field of 2kV/cm for 1h.

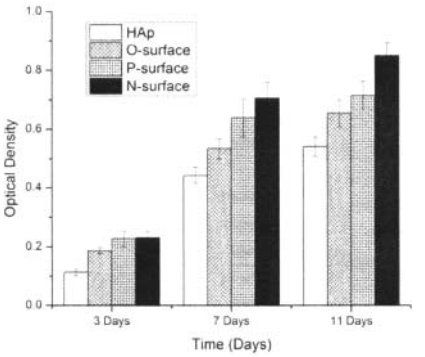

Figure 3. . MTT results of pure and doped HAp (unpolarized, N- and P-surfaces) incubated for 3, 7 and 11 days.

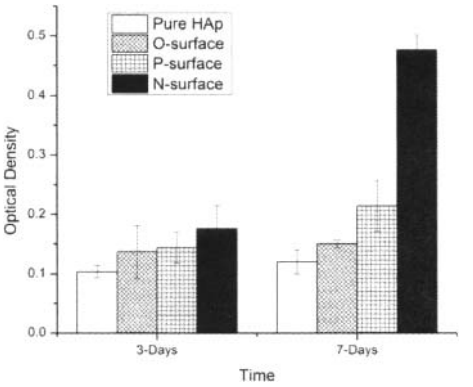

Figure 4. MTT results of pure HAp and doped HAp (unpolarized, N-, and P-surface) incubated for 3 and 7 days.

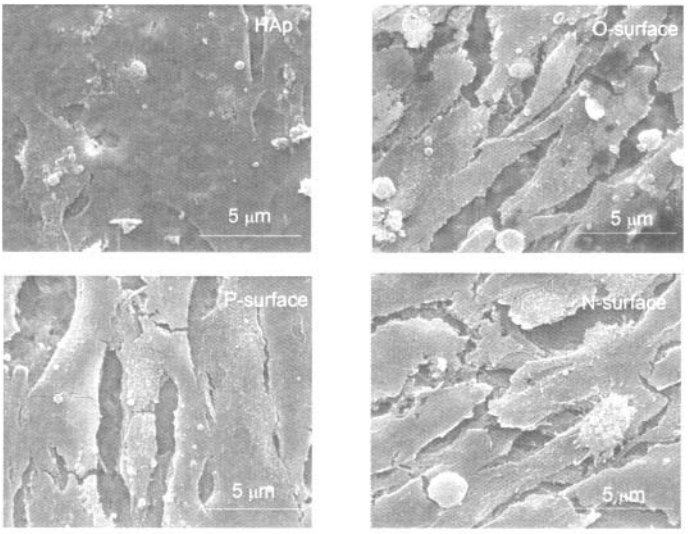

Figure 5. Cell morphology of pure HAp and WO_3 doped HAp surfaces (unpolarized, N-, and P-surface) incubated for 11 days.

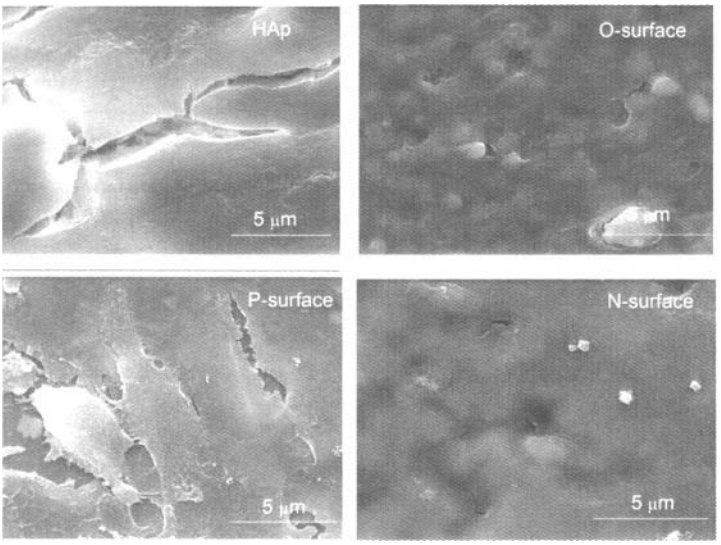

Figure 6. Cell morphology of pure HAp and Ta_2O_5 doped HAp surfaces (unpolarized, N-, and P-surface) incubated for 11 days.